Physics in Collision - Zeuthen, Germany, June 26-28, 2003

MEASUREMENT OF THE ANGLE $\phi_1(\beta)$ AND $B\bar{B}$ MIXING (RECENT RESULTS FROM BaBar AND Belle)

Kazuo Abe
KEK, Tsukuba, Japan 305-0801

ABSTRACT

Recent results from BaBar and Belle experiments on $B\bar{B}$ mixing and $\sin 2\phi_1$ are presented. Accuracy of Δm_d measurements has reached 1.2%. Higher order effects within the Standard Model or possible new physics effect that might appear in the $B\bar{B}$ mixing through non-zero $\Delta\Gamma/\Gamma$, CP violation, or CPT violation have been explored. The BaBar and Belle results on $\sin 2\phi_1$ from the $b \to c\bar{c}s$ modes are in good agreement with each other and a combined result with an accuracy of 8% is in good agreement with a global CKM fit. A simple average of the $\sin 2\phi_1$ values that were measured in the penguin-loop dominated decay modes, ϕK_S, $\eta' K_S$, and $K^+K^-K_S$, shows about 2.5σ deviation from the Standard Model.

1 $e^+e^- \to \Upsilon(4S) \to B\bar{B}$

A scheme of producing Υ(4S) in an asymmetric-energy e^+e^- collisin, that is used at PEP-II and KEKB, enables separation of the decay verteces of the two B mesons. PEP-II operates at 9 GeV $e^- \times$ 3.1 GeV e^+ corresponding to $\Delta z \simeq 260\mu$m, while KEKB operates at 8 GeV $e^- \times 3.5$ GeV e^+ corresponding to $\Delta z \simeq 200\mu$m. Since the size of interaction region in the z direction is much larger than these Δz ($\sim$ 7mm at KEKB), the reference of the proper time must be the decay point of the other B (See Fig. 1). Conservation of charge-conjugation in the $\Upsilon(4\mathrm{S}) \to B^0\bar{B}^0$ decay forces

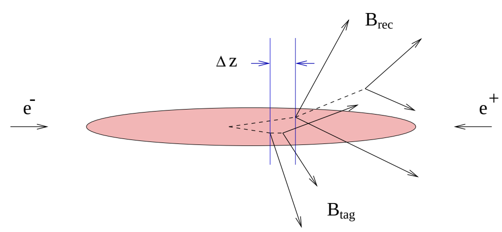

Figure 1: *Schematical drawing of $e^+e^- \to \Upsilon(4\mathrm{S}) \to B\bar{B}$ process at PEP-II and KEKB.*

the time structure of $B\bar{B}$ system to stay as $\psi(t) = |B^0 > |\bar{B}^0 > -|\bar{B}^0 > |B^0 >$ at any t until one B meson decays. This feature is used to determine the flavor of the reconstructed B at $\Delta t = 0$.

2 $B\bar{B}$ Mixing

Mass and flavor eigenstates of the neutral B meson states are expressed by

$$| B_1 >= p \mid B^0 > +q \mid \overline{B^0} >, \quad | B_2 >= p \mid B^0 > -q \mid \overline{B^0} > . \tag{1}$$

Well defined time dependence of (B_1, B_2) and flavor-specific decays of (B^0, $\bar{B}^0$) lead to the $B^0\bar{B}^0$ oscillation. Probabilities of observing the two B mesons as having the opposite-flavor (OF) or having the same-flavor (SF) at Δt are expressed by

$$P^{\mathrm{OF}} \propto \frac{e^{-|\Delta t/\tau_{B^0}|}}{4\tau_{B^0}}\left[1+\cos(\Delta m_d \Delta t)\right], \quad P^{\mathrm{SF}} \propto \frac{e^{-|\Delta t/\tau_{B^0}|}}{4\tau_{B^0}}\left[1-\cos(\Delta m_d \Delta t)\right]. \tag{2}$$

The mixing parameters can be obtained either by reconstructing one B in flavor-specific modes such as $D^{(*)}\pi$, $D^{(*)}\rho$, $D^{(*)}\ell\nu$, and flavor-tagging the other B using information of remaining tracks in the event, or by using dilepton events. For the $\sin 2\phi_1$ measurement, we reconstruct one B as CP eigenstates such as $J/\psi K_S$. The OF-SF asymmetries that were measured by Belle [1] and BaBar [2] are shown in

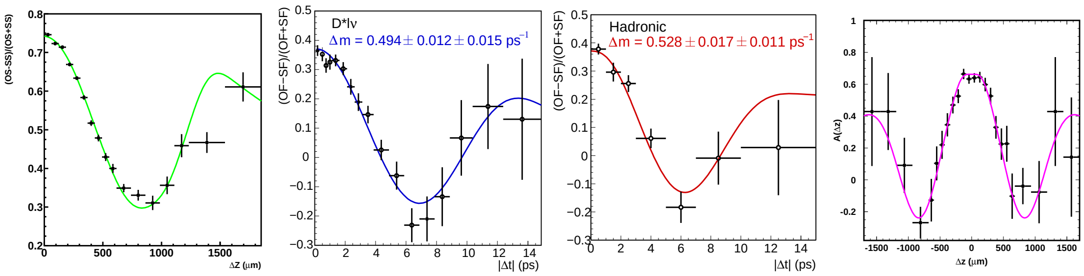

Figure 2: *Belle Δm_d measurements based on 32 million $B\bar{B}$. From left to right, dileptons, semileptonic decays, hadronic decays, and partially reconstructed $D^*\pi$ decays.*

Fig. 2 and 3. The results are summarized in Figure 4. A combined result of BaBar and Belle is $\Delta m_d = 0.504 \pm 0.007$ ps^{-1} which dominates the world average of $\Delta m_d = 0.502 \pm 0.006$ ps^{-1}.

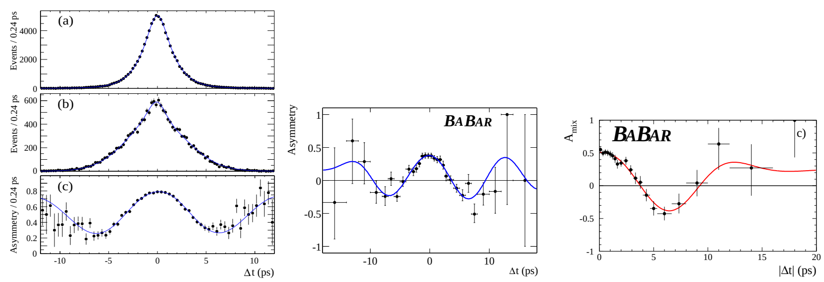

Figure 3: *BaBar Δm_d measurements. From left to right, dileptons (23M $B\bar{B}$), semileptonic decays (23M $B\bar{B}$), hadronic decays (32M $B\bar{B}$).*

3 $B\bar{B}$ mixing in Standard Model

In the Standard Model, box-diagram is responsible for $B\bar{B}$ mixing, and expressed as $\Delta m_d = m_{\rm H} - m_{\rm L} = 2|M_{12}|$ where

$$M_{12} = -\frac{G_F^2 m_W^2 \eta_B m_B B_B f_B^2}{12\pi^2} S_0(m_t^2/m_W^2)(V_{td}^* V_{tb})^2. \tag{3}$$

Here B_1 and B_2 are redefined as $B_{\rm H}$ and $B_{\rm L}$. Extraction of $|V_{td}|$ from Δm_d is dominated by a large uncertainty in $f_{B_d}\sqrt{B_{B_d}} = 230 \pm 40$ MeV [3]. Improved lattice QCD calculations and Δm_s measurements are waited.

The mixing also has an absorptive part $\Delta\Gamma = \Gamma_{\rm L} - \Gamma_{\rm H} = 2|\Gamma_{12}|$, which is tiny in the Standard Model.

$$\left|\frac{\Gamma_{12}}{M_{12}}\right| \sim \frac{\Delta\Gamma}{\Gamma} \simeq \frac{3\pi}{2}\frac{m_b^2}{m_W^2}\frac{1}{S_0(m_t^2/m_W^2)} \sim 5 \times 10^{-3}(\pm 30\%). \tag{4}$$

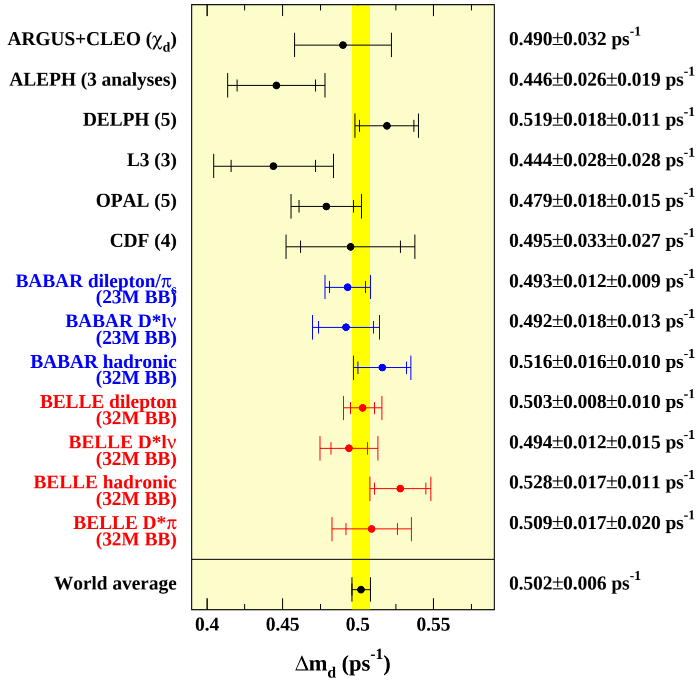

Figure 4: *Present status of Δm_d measurements.*

Any deviation will be difficult to explain in the Standard Model, which of course makes this measurement very interesting. For non-zero $\Delta\Gamma$, the time-dependent decay rates for the flavor-specific state ($B \to f(\bar{f})$) must be modified as

$$[1 \pm \cos(\Delta m_d \Delta t)] \to \left[\cosh \frac{\Delta\Gamma_d \Delta t}{2} \pm \cos(\Delta m \Delta t)\right] \tag{5}$$

while for CP eigenstate ($B^0 \to f_{CP}$, CP-even (CP-odd)), it must be modified as

$$[1 \pm \sin 2\phi_1 \sin(\Delta m_d \Delta t)] \to \left[\cosh \frac{\Delta\Gamma_d \Delta t}{2} \mp \cos 2\phi_1 \sinh \frac{\Delta\Gamma_d \Delta t}{2} \pm \sin 2\phi_1 \sin(\Delta m \Delta t)\right]. \tag{6}$$

CP violation in the $B\bar{B}$ mixing leads to $|q/p| \neq 1$ and it is related to Γ_{12} and M_{12} as

$$1 - |\frac{q}{p}|^2 \simeq Im\left(\frac{\Gamma_{12}}{M_{12}}\right). \tag{7}$$

In the Standard Model, $|q/p|$ is less than 10^{-3} because $|\Gamma_{12}/M_{12}| \sim 5 \times 10^{-3}$ and $\phi_{M_{12}} - \phi_{\Gamma_{12}} = \pi + O(m_c^2/m_b^2)$. Probabilities of observing the SF events are given for ++ and – combinations separately by $P^{\rm SF}_{++} = |p/q|^2 \cdot P^{\rm SF}$ and $P^{\rm SF}_{--} = |q/p|^2 \cdot P^{\rm SF}$. Thus a charge asymmetry in the SF events appears if CP is violated.

CPT violation leads to $p \neq p'$ and/or $q \neq q'$ where the B meson states are described by $\mid B_H >= p \mid B^0 > +q \mid \overline{B^0} >$, $\quad \mid B_L >= p' \mid B^0 > -q' \mid \overline{B^0} >$. We introduce variables θ and ϕ where $q/p = \tan(\frac{\theta}{2})e^{i\phi}$, and $q'/p' = \cot(\frac{\theta}{2})e^{i\phi}$. The time dependence of the OF decay is modified as

$$1+\cos(\Delta m_d \Delta t) \rightarrow [1+|\cos\theta|^2+(1-|\cos\theta|^2)\cos(\Delta m_d \Delta t)-2Im(\cos\theta)\sin(\Delta m_d \Delta t)]. \tag{8}$$

A time-dependent asymmetry in the OF events can appear if CPT is violated [4].

4 Results of $\Delta\Gamma/\Gamma$, $|q/p|$, $\cos\theta$

BaBar has performed a global fit to the fully reconstructed hadronic events from the 88M $B\bar{B}$ sample and extracted $\Delta\Gamma/\Gamma$, $|q/p|$, $Re(\cos\theta)$, and $Im(\cos\theta)$ [5]. BaBar also obtained $|q/p|$ from the dilepton events in the 23M $B\bar{B}$ sample [6]. Belle determined $Im(\cos\theta)$ and $Re(\cos\theta)$ using the dilepton events in the 32M $B\bar{B}$ sample [1]. Results are summarized in Table 1.

Table 1: *Results of* $\Delta\Gamma/\Gamma$*,* $|q/p|$*,* $\cos\theta$*. The parameter* z *is equivalent to* $\cos\theta$*.* $\mathrm{sgn}(\mathrm{Re}\lambda_{CP}) = +1$ *in SM.* $\mathrm{Re}\lambda_{CP}/|\lambda_{CP}| \simeq 0.672 \pm 0.068$*.*

	data	variables	result
BaBar	hadronic	$\mathrm{sgn}(\mathrm{Re}\lambda_{CP})\Delta\Gamma/\Gamma$	$-0.008 \pm 0.037 \pm 0.018$
		$\lvert q/p \rvert$	$1.029 \pm 0.013 \pm 0.011$
		$\mathrm{Re}\lambda_{CP}/\lvert\lambda_{CP}\rvert\mathrm{Re}z$	$0.014 \pm 0.035 \pm 0.034$
		$\mathrm{Im}z$	$0.038 \pm 0.029 \pm 0.025$
BaBar	dileptons	$\lvert q/p \rvert$	$0.998 \pm 0.005 \pm 0.007$
Belle	dileptons	$\mathrm{Im}(\cos\theta)$	$0.03 \pm 0.01 \pm 0.03$
		$\mathrm{Re}(\cos\theta)$	$0.00 \pm 0.12 \pm 0.01$

5 $\sin 2\phi_1$ from $J/\psi K_S$ and other $b \rightarrow c\bar{c}s$ decays

Asymmetry of time-dependent decay rates between $(B^0 \rightarrow f)$ and $(\bar{B}^0 \rightarrow \bar{f})$ for the final state $f = \bar{f} = f_{CP}$ is expressed by

$$a_f(t) = \frac{\Gamma(\bar{B}^0(t) \rightarrow f) - \Gamma(B^0(t) \rightarrow f)}{\Gamma(\bar{B}^0(t) \rightarrow f) + \Gamma(B^0(t) \rightarrow f)} = \frac{2Im\lambda_f}{|\lambda_f|^2+1}\sin(\Delta m t) + \frac{|\lambda_f|^2-1}{|\lambda_f|^2+1}\cos(\Delta m t). \tag{9}$$

Information of CP violation is in a quantity λ_f. Namely $Im\lambda_f \neq 0$ results in mixing-assisted CP violation, and $|\lambda_f| \neq 1$ results in direct CP violation. The λ_f is defined

as $\lambda_f = (q/p)\times < f|H|\bar{B}^0 > / < f|H|B^0 >$ where the $B\bar{B}$ mixing contribution is given by $q/p = (V_{tb}^* V_{td})/(V_{tb} V_{td}^*)$ which is equal to $e^{-2i\phi_1}$ in the Standard Model.

For the $J/\psi K_S$ final state (Fig. 5 followed by $K^0 \to K_S$), λ is given by

$$\lambda(J/\psi K_S) = \frac{V_{tb}^* V_{td}}{V_{tb} V_{td}^*} \cdot \eta_{J\psi K_S} \cdot (\frac{V_{cb} V_{cs}^*}{V_{cb}^* V_{cs}}) \cdot (\frac{V_{cd}^* V_{cs}}{V_{cs}^* V_{cd}}). \tag{10}$$

Here η_f is CP eigenvalue of the f state. We obtain $Im\lambda(J/\psi K_S) = \sin 2\phi_1$ and $Im\lambda(J/\psi K_L) = -\sin 2\phi_1$.

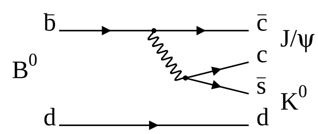

Figure 5: *Diagram for $B^0 \to J/\psi K_S$.*

Methods for the event selections are given in detail in references [7] and [8]. The results presented here are based on the data set of 88M $B\bar{B}$ for BaBar and 85M $B\bar{B}$ for Belle. Both group used $J/\psi K_S$, $\psi' K_S$, $\chi_{c1} K_S$, $\eta_c K_S$, $J/\psi K^*$, and $J/\psi K_L$ final states. Except for the $J/\psi K_L$ final state, the candidate events peak in the mass distributions for reconstructed B mesons. For the $J/\psi K_L$ events, two-body decay of B must be assumed since the K_L energy cannot be detected. BaBar uses the energy-difference, ΔE, between reconstructed B and beam energy, whereas Belle uses the center-of-mass momentum of reconstructed B, p_B^*. They are shown in Fig. 6.

Extraction of $\sin 2\phi_1$ from the Δt distributions are done by maximize a likelihood $L = \prod_i P_i$ (i $\cdots$each candidate event). The probability of each candidate event is described by

$$P_i = \int [f_{\rm sig} P_{\rm sig}(\Delta t') R_{\rm sig}(\Delta t - \Delta t') + (1 - f_{\rm sig}) P_{\rm bkg}(\Delta t') R_{\rm bkg}(\Delta t - \Delta t')]\, d\Delta t' \tag{11}$$

where $f_{\rm sig}$ is signal fraction of candidate event, $P_{\rm sig}$ and $P_{\rm bkg}$ are the probability density functions, and $R_{\rm sig}$ and $R_{\rm bkg}$ are the Δt resolutions. The Δt distributions and asymmetries are shown in Fig. 7 together with their fit results.

The BaBar results are $\sin 2\phi_1 = 0.741 \pm 0.067 \pm 0.034$ and $|\lambda| = 0.948 \pm 0.051 \pm 0.030$, while the Belle results are $\sin 2\phi_1 = 0.719 \pm 0.074 \pm 0.035$ and $|\lambda| = 0.950 \pm 0.049 \pm 0.025$. A combined result is $\sin 2\phi_1 = 0.734 \pm 0.055$. Fig. 8 shows an allowed region of (ρ-η) plane from the $\sin 2\phi_1$ measurement and from a global CKM fit without using $\sin 2\phi_1$. Agreement is excellent.

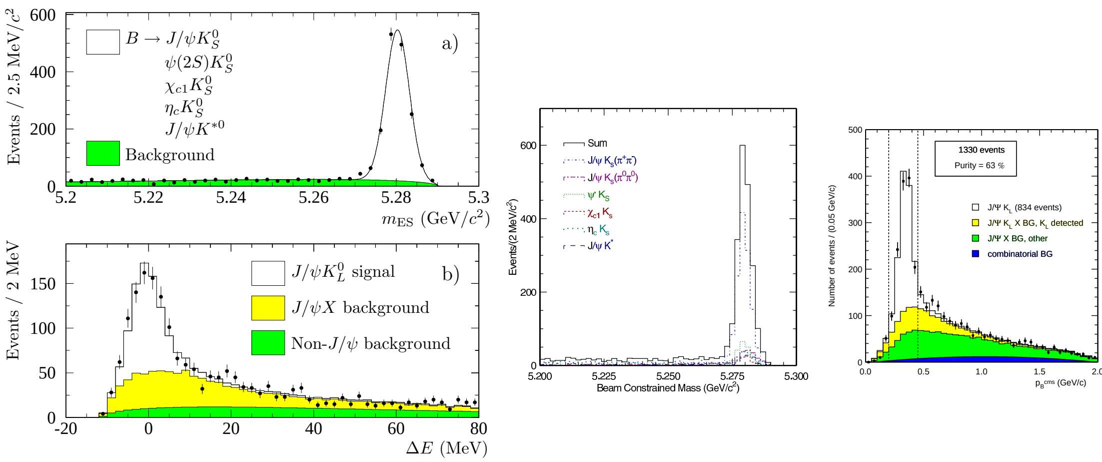

Figure 6: *(Left) Beam-energy substituted mass distribution for the $\eta_{CP} = -1$ final states and ΔE distribution for the $J/\psi K_L$ final state for BaBar. (Right) Beam-energy substituted mass distribution for the $\eta_{CP} = -1$ final states and p_B^* distribution for the $J/\psi K_L$ final state for Belle.*

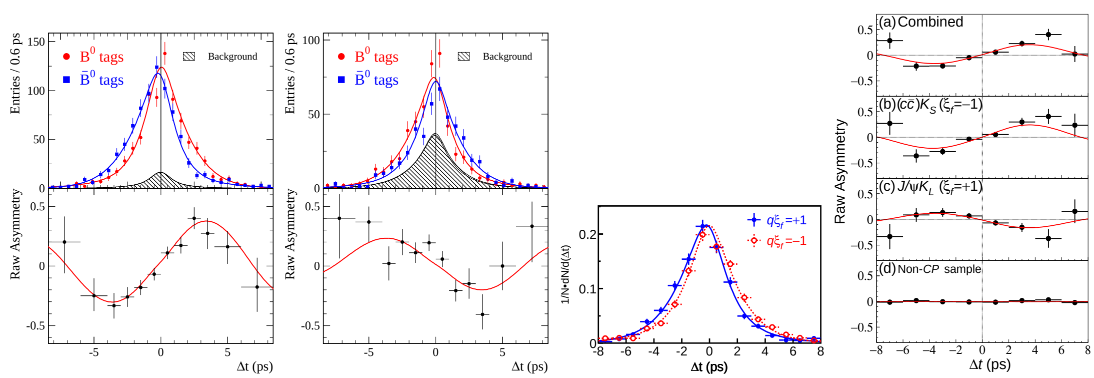

Figure 7: *BaBar Δt distributions and asymmetries for CP-odd final states (far-left) and $J/\psi K_L$ state (2nd-left). Belle Δt distributions for a sum of B^0-tagged $J/\psi K_L$ and $\overline{B^0}$-tagged CP-odd states (labeled as $q\xi_f = +1$) and for a sum of $\overline{B^0}$-tagged $J/\psi K_L$ and B^0-tagged CP-odd states (labeled as $q\xi_f = -1$) (2nd-right). Far-right are Belle asymmetries for $q\xi_f = +1$ and $q\xi_f = - + 1$ samples combined (a), each separately (b) and (c), and for non-CP sample (d).*

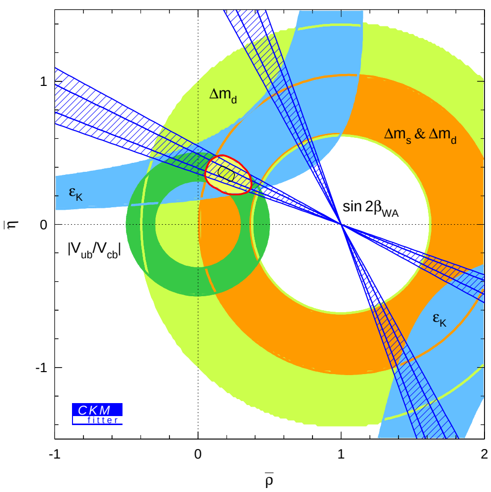

Figure 8: *Shaded area are for 1σ and 2σ regions from the BaBar-Belle combined value of* $\sin 2\phi_1$. *90% (5%) CL contours from a global CKM fit are also shown.*

6 $\sin 2\phi_1$ from loop diagram decays

6.1 ϕK_S

The $B^0 \to \phi K_S$ decay has only $b \to s s \bar{s}$ penguin contribution in the Standard Model (Fig. 9). Leading term has a CKM factor of $V_{cb}V_{cs}^*(P_c - P_t) = A\lambda^2(P_c - P_t)$, where

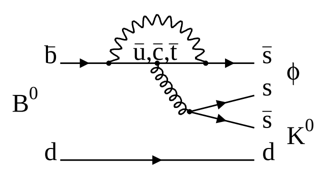

Figure 9: *Standard Model contribution to* $B^0 \to \phi K_S$.

P_q are the penguin amplitudes. This is same as the CKM factor for $B^0 \to J/\psi K_S$. Next-to-leading term $V_{ub}V_{us}^*(P_u - P_t) = A\lambda^4(\rho - i\eta)(P_u - P_t)$ has a different phase, but is suppressed by $\lambda^2 \simeq 5\%$. Since $\eta_{\phi K_S} = -1$, $\sin 2\phi_1$ measured in this mode should be the same as that for the $J/\psi K_S$ in the Standard Model. In order to allow room for new physics, we parameterize the asymmetry distribution by

$$a_f(\Delta t) = S_f \sin(\Delta m_d \Delta t) + A_f \cos(\Delta m_d \Delta t) \tag{12}$$

where

$$S_f = \frac{2Im\lambda_f}{|\lambda_f|^2 + 1}(\simeq -\eta_f \sin 2\phi_1 \text{ in SM}), \quad A_f = -C_f = \frac{|\lambda_f|^2 - 1}{|\lambda_f|^2 + 1}(\simeq 0 \text{ in SM}). \tag{13}$$

Any deviation would be an indication of new physics in penguin loop.

The BaBar results based on 84M $B\bar{B}$ [9] are $S_{\phi K_S} = -0.18 \pm 0.51 \pm 0.07$ and $A_{\phi K_S} = +0.80 \pm 0.38 \pm 0.12$, whereas the Belle results based on 85M $B\bar{B}$ [10] are $S_{\phi K_S} = -0.73 \pm 0.64 \pm 0.22$ and $A_{\phi K_S} = -0.56 \pm 0.41 \pm 0.16$.

6.2 $\eta' K_S$

This mode is contributed by $b \to s s \bar{s}$ penguin, $b \to s d \bar{d}$ penguin, and $b \to u$ tree diagrams (Fig. 10). In the Standard Model, presence of additional $b \to s d \bar{d}$ penguin

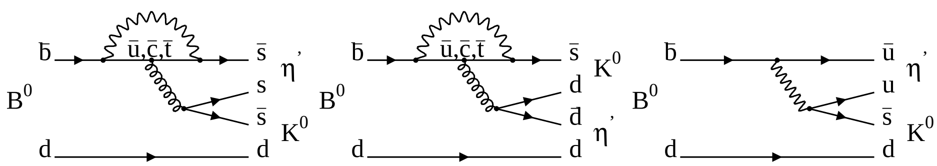

Figure 10: *Standard Model contributions to* $B^0 \to \eta' K_S$.

does not cause any change from the ϕK_S case, and only difference is the additional $b \to u$ tree diagram which is only 5% effect. Since $\eta_{\eta' K_S} = -1$, we expect to have $S_f \simeq \sin 2\phi_1$.

The BaBar results based on 88.9M $B\bar{B}$ [11] are $S_{\eta' K_S} = +0.02 \pm 0.34 \pm 0.03 b$ and $A_{\eta' K_S} = -0.10 \pm 0.23 \pm 0.03$, whereas the Belle results based on 85M $B\bar{B}$ [10] are $S_{\eta' K_S} = +0.71 \pm 0.37^{+0.05}_{0.06}$ and $A_{\eta' K_S} = +0.26 \pm 0.22 \pm 0.03$.

6.3 $K^+ K^- K_S$

This decay is contributed by $b \to s$ penguin and $b \to u$ tree diagrams (Fig. 11). The Belle analysis for this decay mode shows that the $b \to u$ tree contribution

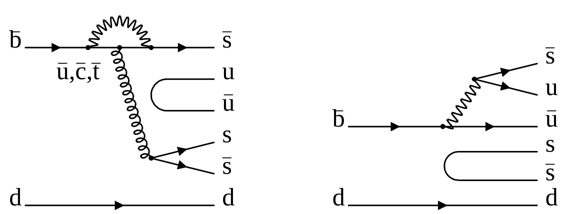

Figure 11: *Standard Model contributions to* $B^0 \to K^+ K^- K_S$.

is negligible and furthermore CP content of the final state is predominantly even ($\eta_{K^+ K^- K_S} = +1$) [10]. Therefore we expect $S_f \simeq -\sin 2\phi_1$. The results based on 85M $B\bar{B}$ are $S_{K^+ K^- K_S} = -0.49 \pm 0.43 \pm 0.11$ and $A_{K^+ K^- K_S} = -0.40 \pm 0.33 \pm 0.10$.

Fig. 12 summarizes the $(-\eta_f S_f)$ measurements for the penguin loop decays. An average "$\sin 2\phi_1$" of those three penguin decays is 0.19 ± 0.20, about 2.5σ off the

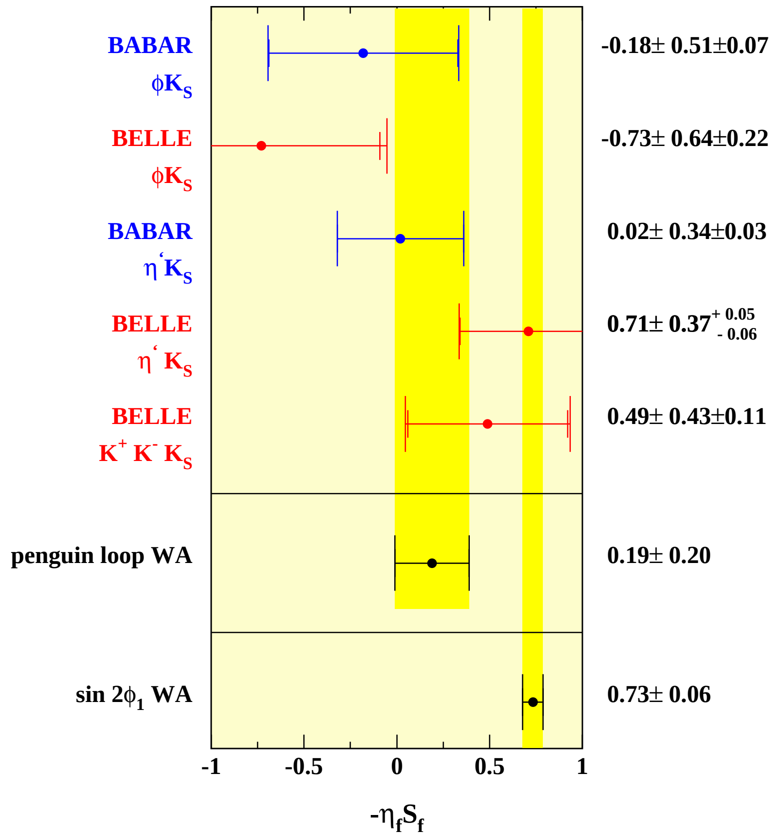

Figure 12: *Summary of $-\eta_f S_f$ measurements for the penguin loop decays.*

Standard Model. We are entering an exciting era for exploring new physics through $\sin 2\phi_1$ measurements in different decay modes.

7 $\sin 2\phi_1$ from other modes

7.1 $J/\psi\pi^0$

In this mode, the tree and penguin contributions are of comparable size(Fig. 13). The CKM factors are $V_{cb}V_{cd}^* = -A\lambda^3$ for the tree, and $V_{cb}V_{cd}^*(P_c - P_t) = -A\lambda^3(P_c - P_t)$ and $V_{ub}V_{ud}^*(P_u - P_t) = A\lambda^3(\rho - i\eta)(P_u - P_t)$ for the penguins, respectively. In an

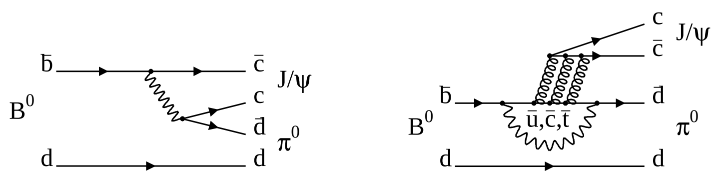

Figure 13: *Standard Model contributions to $B^0 \to J/\psi\pi^0$.*

extreme case of ignoring the penguin, we obtain $S_f \simeq -\sin 2\phi_1$ since $\eta_{J/\psi\pi^0} = +1$. If a deviation is seen, presence of penguin should be suspected first. The BaBar results based on 88M $B\bar{B}$ [12] are $S_{J/\psi\pi^0} = +0.05 \pm 0.49 \pm 0.16$ and $A_{J/\psi\pi^0} = -0.38 \pm 0.41 \pm 0.09$, whereas the Belle results based on 85M $B\bar{B}$ [13] are $S_{J/\psi\pi^0} = -0.93 \pm 0.49 \pm 0.08$ and $A_{J/\psi\pi^0} = -0.25 \pm 0.39 \pm 0.06$.

7.2 $D^{*+}D^{*-}$ and $D^{*+}D^-$

These modes have similar "penguin pollution" as $J/\psi\pi^0$ (Fig. 14). The CKM factors are $V_{cb}V_{cd}^* = -A\lambda^3$ for the tree, and $V_{cb}V_{cd}^*(P_c - P_u) = -A\lambda^3(P_c - P_u)$ and $V_{tb}V_{td}^*(P_t - P_u) = A\lambda^3(1-\rho+i\eta)(P_t - P_u)$ for the penguins, respectively. BaBar angular

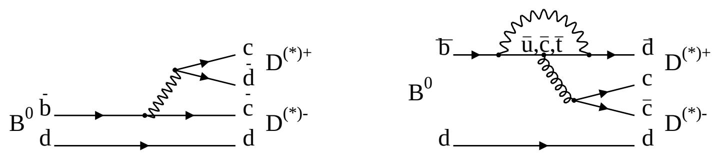

Figure 14: *Standard Model contributions to $B^0 \to D^{(*)+}D^{(*)-}$.*

analysis [15] showed that CP content of the $D^{*+}D^{*-}$ final state is predominantly even ($\eta_{D^{*+}D^{*-}} \simeq +1$). In an extreme case of ignorin the penguin, we obtain $S_f \simeq -\sin 2\phi_1$. The $D^{*+}D^-$ final state is not a CP eigenstate. In an extreme case of ignoring the penguin, we obtain $S_f^{\pm} = S_f^{\mp} \simeq -\sin 2\phi_1$. The BaBar results based on 88M $B\bar{B}$ [14] are

$$\begin{aligned} S^{\pm}_{D^*D} &= -0.24 \pm 0.69 \pm 0.12, \quad S^{\mp}_{D^*D} = -0.82 \pm 0.75 \pm 0.14 \\ A^{\pm}_{D^*D} &= +0.22 \pm 0.37 \pm 0.10, \quad A^{\mp}_{D^*D} = +0.47 \pm 0.40 \pm 0.12. \end{aligned} \tag{14}$$

8 Summary

Precision of Δm_d has reached 1.2%. Attempt for observing higher order effect and possible new physics effects in $B\bar{B}$ mixing are vigorously explored. The Δm_d measurements are an important testing ground for the Δt measurement and flavor-tagging. Precision of $\sin 2\phi_1$ has reached 8%. Statistical error still dominates. It is in good agreement with a global CKM fit (without $\sin 2\phi_1$). $|\lambda|$ is consistent with 1 in $b \to c\bar{c}s$ decays as expected in the Standard Model. New physics search by "$\sin 2\phi_1$" measurements in penguin loops is well under way. "$\sin 2\phi_1$" measurements for "penguin polluted" decays were also pushed to find useful information.

References

1. N. Hasting *et al.*, Phys. Rev. D **67**, 052004 (2003); K. Hara *et al.*, Phys. Rev. Lett. **89**, 251803 (2002); T. Tomura *et al.*, Phys. Lett. **B542** 207 (2002); Y. Zheng *et al.*, Phys. Rev D **67**, 092004 (2003).

2. B. Aubert *et al.* Phys. Rev. Lett. **88**, 221803 (2002); B. Aubert *et al.* Phys. Rev. Lett. **88**, 221802 (2002); B. Aubert *et al*, hep-ex/0212017.

3. K. Hagiwara *et al.* (Particle Data Group), Phys. Rev. D **66**, 010001 (2002).

4. See, for example, A. Mohapatra, M. Satpathy, K. Abe, and Y. Sakai, Phys. Rev. D **58**, 036003 (1998).

5. hep-ex/0303043.

6. B. Aubert *et al.*, Phys. Rev. Lett. **88**, 231801 (2002).

7. B. Aubert *et al.* Phys. Rev. Lett. **89**, 201802 (2002).

8. K. Abe *et al.* Phys. Rev. D **66**, 071102 (2002).

9. Talk presented at Moriond Conference (March 2003).

10. K. Abe *et al.* Phys. Rev. D **67**, 031102(R) (2003).

11. B. Aubert *et al.* hep-ex/0303046.

12. B. Aubert *et al.* hep-ex/0303018.

13. K. Abe *et al.* Belle-CONF-0201.

14. B. Aubert *et al.* hep-ex/0303004.

15. Talk presented at FPCP (June 2003).